



Samarium doped KMgBO_3 phosphors for orange-red light emission

B. SIVA KUMAR^{1a*}, H. UMAMAHESVARI^{2*}, K. THYAGARAJAN^{1b*}

^{1a&1b}Department of Physics, JNTUA College of Engineering Kalikiri, Constituent College of Jawaharlal Nehru Technological University Anantapur, Anantapuramu - 515 002, A.P, India

²Department of Physics, Sreenivasa Institute of Technology and Management Studies (Autonomous), Chittoor-517 127, Affiliated to Jawaharlal Nehru Technological University Anantapur, Ananthapuramu, A.P, India.

Abstract

To improve orange-red color releasing phosphor material with white light emitting diodes (W-LEDs), 2mol%, 4mol%, 6mol% and 8 mol% of Sm^{3+} ion doped in KMgBO_3 phosphor materials were made up with solid state technique. Their structural, morphological, optical along with emission characteristics of produced powders have been studied using XRD, FTIR, SEM, UV-Vis-NIR spectrometer along with fluorescence spectrometer. This XRD spectrum shows the crystal structure of $\text{KMgBO}_3: \text{Sm}^{3+}$ phosphors are single phase cubic through $P2_13$ space group. From excitation spectra, the prominent excitation band observed at ${}^6\text{H}_{5/2} \rightarrow {}^4\text{F}_{7/2}$, this transition has been utilized to get emission spectra. The emission spectra consist of ${}^4\text{G}_{5/2} \rightarrow {}^6\text{H}_{5/2}$, ${}^6\text{H}_{7/2}$ and ${}^6\text{H}_{9/2}$ transitions corresponding to the Sm^{3+} ion. This intense emissions band was noticed on ${}^4\text{G}_{5/2} \rightarrow {}^6\text{H}_{7/2}$ among all these luminescence transitions. The CIE, CCT and decay life time values were computed and analyzed. All of these findings strongly suggested the produced phosphor materials are useful for orange-red color emission component in W-LEDs along with displaying devices.

Keywords: Solid-state technique; Rare earths; Emission spectra; CIE; KMgBO_3 phosphor materials.

Introduction

A material which shows luminescence is typically called as phosphors. It is synthesized by activating the rare-earth (RE) along with transition elements. Phosphors recently ignited scientific attention owing to its vast variety of uses [1, 2]. RE-doped materials have been significantly investigated owing to its favourable spectroscopic characteristics, such as tuneable emission, brightness, high Stokes change, substantial emission efficacy and long emission lifetime [3, 4]. These properties frame RE-doped materials utilized in amplifiers,

optical temperature sensing, lasers, cells of solar, detection of x-rays, communication devices, panels of display, medical research and storage of energy devices [5-9].

Due to f-f transitions of several discrete energy levels, RE doped phosphors generally display sharp radiation over a large spectrum. Based on the host matrix, with RE ions functioning as catalysts or detectors[10]. Several investigations have already initiated using various strategies to enhance the luminous behaviour of RE doped phosphors. [6, 11]. In fact, the phosphor's luminous centres, structures, and components have a significant impact on the colour, intensity, and luminous efficiency [10, 12, 13].

When selecting acceptable hosts and dopants, it were noticed the structure of crystals, ionic radii, conductivity of heat, light efficacy, refractive index, and phonon frequencies become important considerations since particular phosphors' distinctive compositions make them more helpful. [14,15].

Because of its great intensity, small size, energy savings, extended lifespan, and excellent colour rendering index (CRI), solid-state WLEDs have attracted attention [2, 10, 12]. Because of all of these features, WLEDs have mostly replaced traditional luminescent and incandescence bulbs [16]. WLEDs are often created by combining different colours generated by multichip LEDs to WLEDs using phosphors. [17]. The latter process produces what are known as phosphor transformed WLEDs, which possess high CRI readings and constitute almost all of commonly accessible WLEDs. The resultant features of emitting phosphors were required to make WLEDs and their light applications. For instance, Sreeja et al. investigated that Eu^{3+} ions doped Ba_2CaWO_6 [17] and Pr^{3+} doped Ba_2CaWO_6 [18] phosphors may emit white light effectively. In addition, ZhenghuaJu et al. researched Eu^{3+} and Sm^{3+} activated SrWO_4 phosphors for usage on W-LEDs [19, 20], while D. Singh et al. investigated Eu^{3+} and RE^{3+} stimulated SrAl_2O_4 Green nano phosphors for display device applications [21]. Wang et al. [22] additionally released more important investigations on a variety of WLED phosphors. This study's long-term goal is to find RE ion triggered phosphors as luminous materials that have significant quantum efficiency. Samarium stands out among all RE ions because its $^4\text{G}_{5/2}$ - transmitting level has high quantum efficiency as well as variety of emission-quenching routes [23, 24]. The considerable energy gaping (7000 cm^{-1}) over the Sm^{3+} levels $^4\text{G}_{5/2}$ as well as $^6\text{F}_{11/2}$ supports reducing non-radiative decay [25]. Sm^{3+} ions often produce reddish-orange light owing to electronic shifts involving the excitation state $^4\text{G}_{5/2} \rightarrow ^6\text{H}_{5/2}$, $^6\text{H}_{7/2}$, $^6\text{H}_{9/2}$ and $^6\text{H}_{11/2}$ [26, 27].

In accordance to research literature, Sm^{3+} ion doped phosphors have a high number of visible light output channels, allowing them to be used in LEDs, tuneable lasers, optical devices for communication, and devices for displaying [25-28]. Any suitable host material must be selected to produce the effective emission of white light phosphors. Actually, oxide hosts are both physically as well as chemically reliable to the relevance borates owing to dynamic luminous characteristics as well as diverse crystalline structure [29,30]. Alkaline-earth borates material technological recognised for the light emissions. In this regard, Ce^{3+} triggered NaSrBO_3 [31] is used for blue light Tb^{3+} triggered $\text{Sr}_2\text{B}_2\text{O}_5$ [32] and Ce^{3+} triggered NaBaBO_3 [33] are used for green emissions and $\text{LiSr}_4(\text{BO}_3)_3$ added with Sm^{3+} [34] phosphors are being proposed to be exciting luminous materials. There are no publications about the structure their nature, optic performance as well as luminescence abilities of Sm^{3+} triggered KMgBO_3 (KMB) phosphor material based on a review of the literature. The process, structural their nature, optical performance, and emission features of Sm^{3+} triggered KMgBO_3 phosphors synthesised utilising a solid state approach are described in this study. The geometrical nature, optic performance, radiation performance, stimulated condition as well as decay life time features for the produced phosphors got thoroughly investigated.

Exploratory Section

Solid state approach was adopted for creating the 2mol%, 4mol%, 6mol% and 8 mol% of Sm^{3+} ion doped in KMgBO_3 phosphor materials. Initial substances contained higher purity powdered of H_3BO_3 , MgO , K_2CO_3 , and Sm_2O_3 . Depending on the balanced relationship, the matching starting components were weighed and combined with help of small of quantity of acetone before being crushed in a mortar of agate for a sixty-minute period to achieve homogeneity. Which were heated for a period of 120 minutes in a crucible made of porcelain at a temperature of 200 °C. The phosphor grains then crushed for another thirty-minute period before being put in a crucible made of porcelain that was heated at 700 °C using a muffle oven for a period of five hours. The collected samples were thoroughly cooled to lab temperature and examined. X-ray diffraction characteristics of 2mol%, 4mol%, 6mol% and 8 mol% of Sm^{3+} ion doped in KMgBO_3 phosphor materials were obtained with the help of Bragg-Brentano configuration of Shimadzu XRD-6000 diffraction meter. In this as detector Cu_α source of x-rays a counter for scintillation and nickel made filter to blocking K_β emissions. Shimadzu tracer-100 FTIR spectrometer with ATR Diamond attachments was used to get the 600-4000 cm^{-1} range of IR spectra phosphors. Scanning electron microscope (SEM, S-4800) applied to investigate

the surface of phosphor materials. The reflectance spectra of diffusion have been gathered using the UV-Vis-NIR spectrophotometer (Varian: 5000).

The excitation, emission and decay curves were recording using xenon lamp (450 W) of EDIN-BURGH FLS980 fluorescence spectrometer.

Discussion & Outcomes

Crystal structure

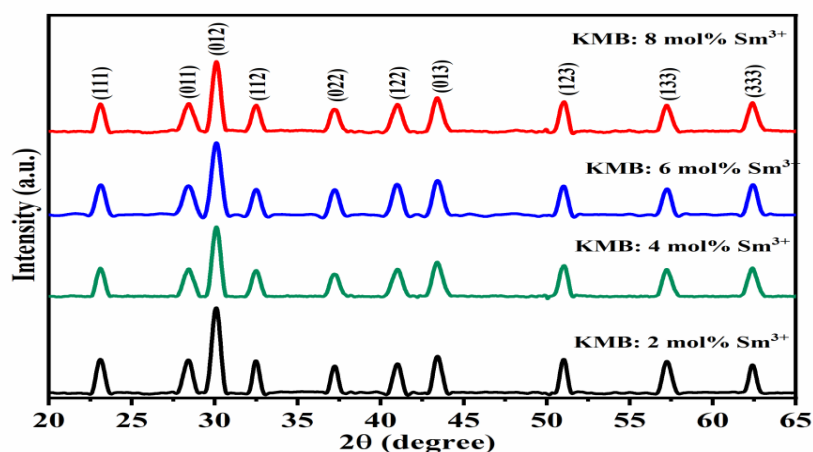


Fig.1. XRD spectrum of sm^{3+} doped KMgBO_3 phosphor powders

The X-ray diffraction spectrum of solid state developed 2mol%, 4mol%, 6mol% and 8 mol% of Sm^{3+} ion doped in KMgBO_3 phosphor materials displayed in Fig. 1. In this bands of distribution were equivalent of Inorganic Crystal Structure Database (ICSD) no. 174336 with no any extra peaks.

This findings proved that the existing phosphor powders constitute single phased, perfect cubic crystal with the $P2_13$ space group as their structure and their lattice constant $a = b = c = 6.8344$ [35]. The miller indices have been utilised to index all of the diffraction spikes.

Eq.1 [36] derives mean crystallite size (D) using the Debye-Scherer's technique.

$$D_{hkl} = k\lambda / [\beta(2\theta) \cos\theta] \quad (1)$$

In which λ denotes X-ray wavelength (1.5405 Å), k denotes constant (0.9), θ denotes diffraction angle of measured profile and β denotes full-width at half maximum (FWHM, in radian). All D values of the 2mol%,

4mol%, 6mol% and 8 mol% of Sm^{3+} ion doped in KMgBO_3 phosphor powders were determined using the significant diffracted peak at (0 1 2) and were found to be 1.140, 1.126, 1.084 & 0.998 μm , accordingly.

Fourier transform infrared spectral analysis

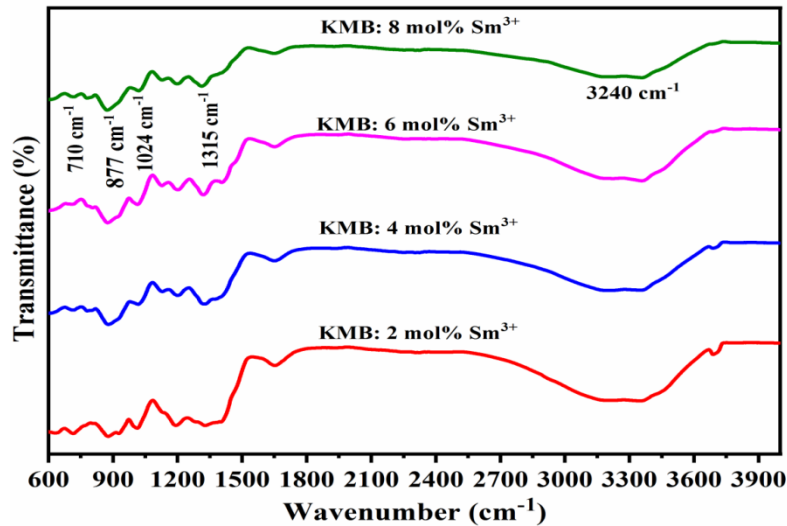


Fig. 2. FTIR spectrum of Sm^{3+} -doped KMB phosphor powders

Because of infrared wavelength (IR) absorption, FTIR shows molecular vibration properties. The intensity of absorption shows how quickly molecules may exchange absorption energy for a change in dipole moment, which in turn causes vibrations in the molecules.

The FTIR spectrum of 2mol%, 4mol%, 6mol% and 8 mol% of Sm^{3+} ion doped in KMgBO_3 phosphor powders were provided in the Fig. 2. The bands of absorption noticed at 2800-3600 cm^{-1} were ascribed to $-\text{OH}$ stretched vibrations of molecule and the spectra was caused by materials absorbing ambient water contents [37]. An absorption band of 1665 cm^{-1} was found to correspond to the asymmetric stretched vibration of B-O bonding. The 1315 cm^{-1} absorbance band has been identified and it is associated with B-O asymmetric stretch vibration. The absorption bands 1024 and 877 cm^{-1} were identified and they are associated with BO_3 trigonal vibrated B-O bonding. Absorbance band were identified in the absorbing peak of 710 cm^{-1} and that was related to Mg/K-O stretches of the Mg/ KO_6 Octahedron [38]. The existence of B-O trigonal BO_3 along with metallic linkages in KMB is confirmed by FTIR spectra.

Morphology analysis

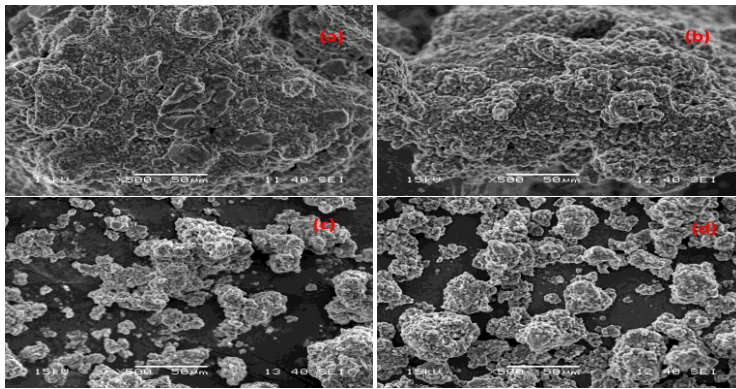


Fig.3. SEM images (a-d) of Sm^{3+} doped KMB phosphor Powders

Fig. 3. display the SEM image (a-d) of 2mol%, 4mol%, 6mol% and 8 mol% of Sm^{3+} ion doped in KMgBO_3 phosphor powders. It denotes uneven morphological features caused by milling the materials during preparation at the elevated temperatures were required to create the phosphor powder. All of the pictures revealed particle sizes ranging from 1 to 4 μm .

Diffuse reflectance analysis

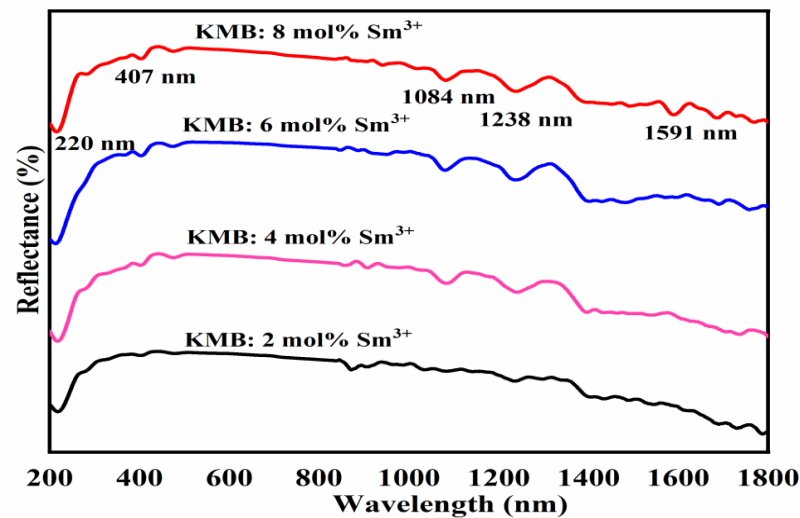


Fig.4. Absorption spectra of Sm^{3+} doped KMB phosphor powders

Fig. 4. exhibits the diffused reflectance spectra (DRS) of 2mol%, 4mol%, 6mol% and 8 mol% of Sm^{3+} ion doped in KMgBO_3 phosphor powders. The absorption spectra revealed that electron transit through a valence band to conduction band induced strong peaks in absorption at 220, 407, 1084, 1238 and 1591 nm. Furthermore, when the concentration of Sm^{3+} ions went up, their absorption peaks changed slightly to appear at lower wavelength (blue shift). From the UV-Vis band, no fragile absorption peaks were noticed in any of the samples, suggesting that surface flaws, traps and contaminants are very low. Applying wood and Tauc's

connection, optical energy gap (E_g) for 2mol%, 4mol%, 6mol% and 8 mol% of Sm^{3+} ion doped in $KMgBO_3$ phosphor powders were computed. As per Eq. 2, E_g is an amalgamation of energy of photons as well as absorption[39].

$$h\nu\alpha \propto (h\nu - E_g)^k \quad (2)$$

Where h denotes Planck's constant, ν denotes frequency, k denotes constant, E_g denotes optic energy gap and α denotes absorbance associated for distinct classes on electronic shifts ($k=1/2, 2, 3/2$ and 3).

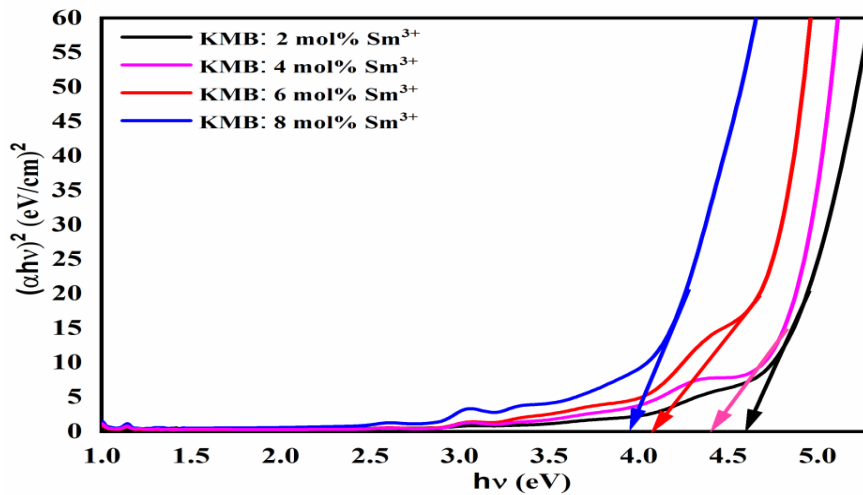


Fig. 5. Tauc's plot of Sm^{3+} doped KMB phosphor powders

As a consequence of scientific evidence indicating the oxides substances having directly permitted electronic shifts, $k=1/2$ was used into conventional Eq. 2. Extrapolation of a straighter portion at its tail either the curve $(h\nu\alpha)^2 = 0$ on the absorbent spectra generated E_g values, displayed on Fig. 5. That predicted E_g readings for 2mol%, 4mol%, 6mol% and 8 mol% of Sm^{3+} ion doped in $KMgBO_3$ phosphor powders given the following chart proved 4.60, 4.41, 4.08 and 3.95 eV respectively. E_g reading reduced as Sm^{3+} concentration grew due to structural flaws. The E_g values dropped as Sm^{3+} concentration grew due to structural flaws like voids and the degree of structure disorder found in the crystalline material, indicating that suited to swapping intermediates in state of energy allocations inside the gap between the bands.

Photoluminescence studies

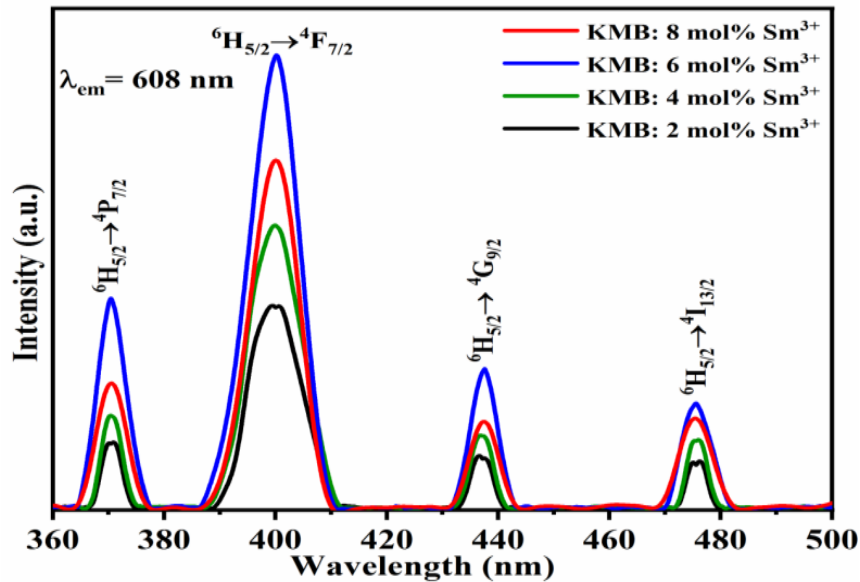


Fig. 6. Excitation spectra of Sm^{3+} doped KMB phosphor powders

Excitation, emissions as well as deteriorated data had been used for exploring the photoluminescence characteristics of 2 mol%, 4 mol%, 6 mol% and 8 mol% of Sm^{3+} ion doped in KMgBO_3 phosphor powders. That excitation spectra were collected tracking emissions on 608 nm associated transition ${}^4\text{G}_{5/2} \rightarrow {}^6\text{H}_{7/2}$ of Sm^{3+} ion can be seen Fig. 6. A sequence of excited bands ranging from the ${}^6\text{H}_{5/2}$ ground level to stimulated energy levels, including ${}^4\text{P}_{7/2}$ (370 nm), ${}^4\text{F}_{7/2}$ (400 nm), ${}^4\text{G}_{9/2}$ (437 nm) and ${}^4\text{I}_{13/2}$ (475 nm) can be displayed in excitation spectra. The excited bands were assigned in accordance with Carnall et al. [40]. The excited spectrum demonstrate the strength for the detected Sm^{3+} excitation lines increases with concentration, exhibiting that Sm^{3+} ions are distributed uniformly. The ${}^6\text{H}_{5/2} \rightarrow {}^4\text{H}_{7/2}$ (400 nm) transition has the greatest amplitude among the reported excitation transitions, therefore the wavelength associated to that transition was utilized to analyze the fluorescence Sm^{3+} ions in KMB phosphor powders.

Emissions spectrum of 2 mol%, 4 mol%, 6 mol% and 8 mol% of Sm^{3+} ion doped in KMgBO_3 phosphor powders obtained by activating with 400 nm (${}^6\text{H}_{5/2} \rightarrow {}^4\text{H}_{7/2}$) xenon flash lighting show Sm^{3+} typical emission peaks in the spectrum area from 550 to 720 nm. The luminescence spectrum of investigated phosphor powders were shown in Fig. 7 after 400 nm excitation. Emission spectrums were allocated for the four Sm^{3+} ion transitions ${}^4\text{G}_{5/2} \rightarrow {}^6\text{H}_{5/2}$ (558 nm), ${}^6\text{H}_{7/2}$ (608 nm), ${}^6\text{H}_{9/2}$ (653 nm) and ${}^6\text{H}_{11/2}$ (708 nm). The amplitude emissions at 608 nm connected with the ${}^4\text{G}_{5/2} \rightarrow {}^6\text{H}_{7/2}$ shift has the maximum strength and it is accountable to the typical orange - red light output with Sm^{3+} ions.

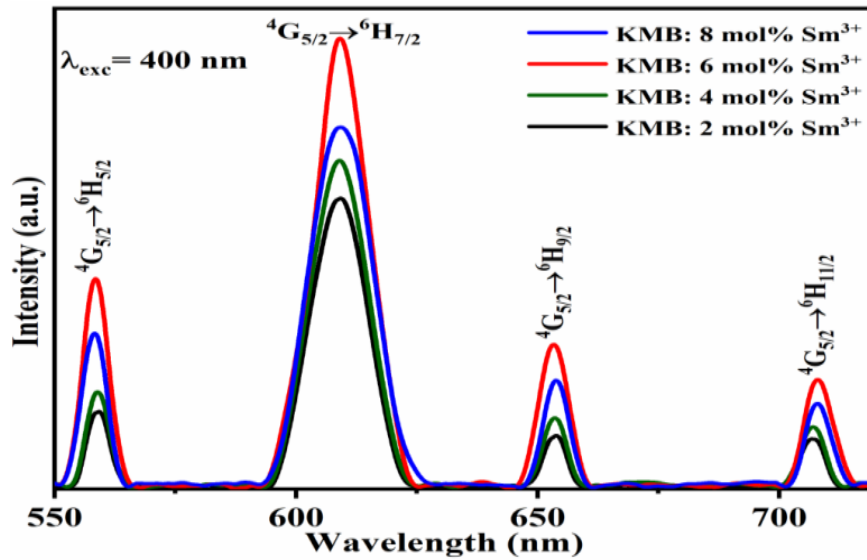


Fig. 7. Emission spectrum of Sm^{3+} doped KMB phosphor powders

The emission spectra, like the excitation spectra, reveal a quenching in photoluminescence brightness above 6 mol% Sm^{3+} concentration of ions. Concentrated quenching on both emission as well as excitation with greater Sm^{3+} ion concentration ($x > 6$ mol%) might be associated the conversion of energy across activated Sm^{3+} ion via relaxation crosswise.

When it comes to Sm^{3+} ion, the transitions ${}^4G_{5/2} \rightarrow {}^6H_{5/2}$ (558 nm), ${}^6H_{7/2}$ (608 nm) were magnetic dipoles ($DJ = 0, \pm 1$), whereas the transitions ${}^4G_{5/2} \rightarrow {}^6H_{9/2}$, ${}^6H_{11/2}$ were electric dipoles ($DJ \leq 6$) [41]. To figure out the precise local symmetries of these Sm^{3+} ions, also a compatible intensity ratio (I_R) between electric dipole with magnetic dipole transformations ($I_R = {}^4G_{5/2} \rightarrow {}^6H_{9/2} / {}^4G_{5/2} \rightarrow {}^6H_{7/2}$) was found. In cases where the I_R magnitude is below one, their Sm^{3+} ions fill the hosting lattice's inversion symmetry positions. If in cases magnitude is above one, their Sm^{3+} ions fill the hosting lattice's non- inversion symmetry positions [42].

The I_R magnitudes in the current study are likely 0.184, 0.218, 0.319 and 0.302 for $x = 2, 4, 6,$ and 8 mol%, accordingly. The tiny (lower than one) value of I_R implies the presence of Sm^{3+} ions reside in the KMB lattice's inversion symmetry locations. The I_R quantities, like excitation and emission spectrum, show concentration quenching.

Emission deterioration

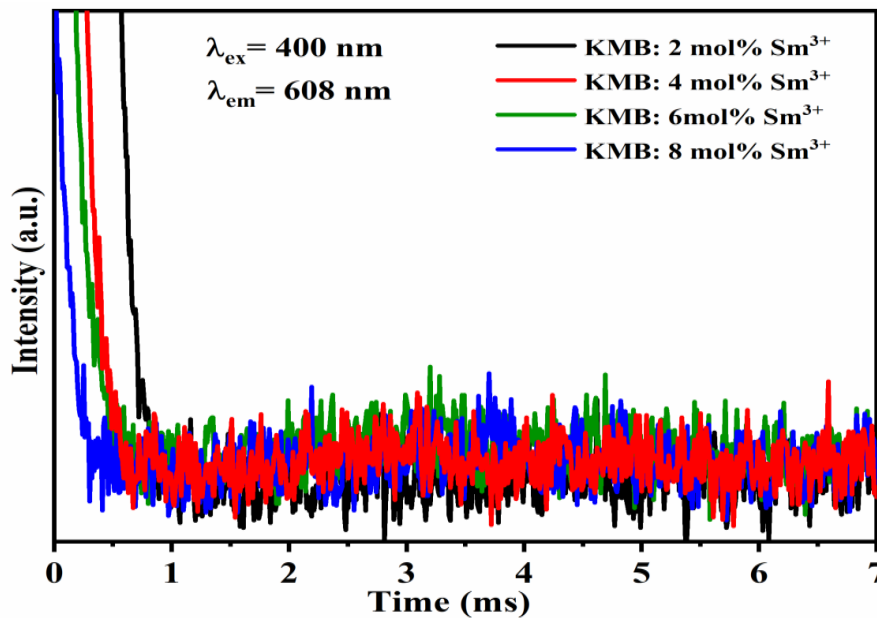


Fig. 8. Emission deterioration curves of Sm^{3+} doped KMB phosphor powders

Emission deterioration caused by the $^4\text{G}_{5/2}$ exciting degree of Sm^{3+} ion in KMB phosphor powders were studied by measuring the emission along with stimulation wavelengths for 608 nm as well 400 nm, accordingly. Fig. 8. exhibits the deteriorate intensity verses time graphs. Each of the deteriorate curves match clearly with a double exponential activities, $I = A_1 e^{\left(\frac{-t}{\tau_1}\right)} + A_2 e^{\left(\frac{-t}{\tau_2}\right)}$, at which I denotes value of intensity with time t, τ_1 as well as τ_2 constitute the exponent life time factors and A_1 and A_2 stored as constants [43]. The period of existence of a specific emission level was calculated by multiplying the initial e –folding by the strength of deteriorate curves. The lifespan values for 2mol%, 4mol%, 6mol% and 8 mol% of Sm^{3+} ion doped in KMgBO_3 phosphor powders comprised, accordingly 0.85, 0.69, 0.57 and 0.38ms. The enhanced interactions among excited Sm^{3+} ions might explain the steady reduction in lifespan with increasing Sm^{3+} concentration. The dampening of fluorescence deterioration at increasing Sm^{3+} ion concentrations ($x > 6$ mol%) is caused mostly by the transmission of energy among the excitation of Sm^{3+} ions via crossed relaxation. When activated at 400 nm, these 2mol%, 4mol%, 6mol% and 8 mol% of Sm^{3+} ion doped in KMgBO_3 phosphor powders display bright orange-red lighting. As a result, the 6mol% Sm^{3+} ion doped KMB phosphor powders is suited for orange-red output in a variety of optical use cases.

Chromaticity coordinates and Correlated color temperature

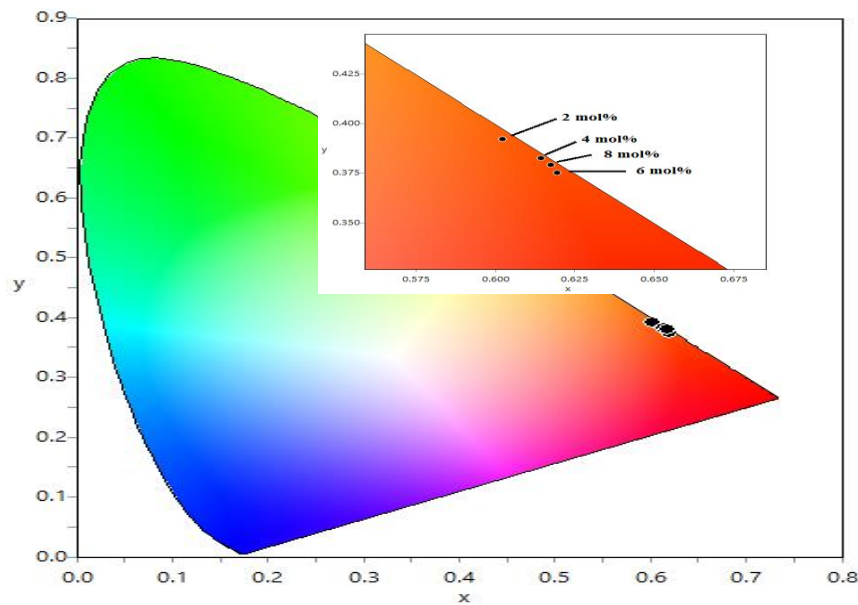


Fig. 9. CIE diagram of Sm^{3+} doped KMB phosphor powders

To look into the color perception as well as emission temperatures for 2mol%, 4mol%, 6mol% and 8 mol% of Sm^{3+} ion doped in KMgBO_3 phosphor powders, this Commission Internationale de l'Eclairage (CIE) 1931 coordinates of chromaticity (x, y) as well as Co-related colour temperature (CCT) were calculated utilizing emission spectrum and are presented in table 1 [44]. All of the CIE coordinates can be identified in this orange-red zone of the CIE map displayed with this Fig.9. These CCT readings showed that the emitted light generally warm.

Table 1. CIE and CCT readings for Sm^{3+} doped KMB phosphor powders

Specimen	CIE (x, y)	CCT (K)
KMB: 2 mol% Sm^{3+}	(0.6022, 0.3920)	1411
KMB: 4 mol% Sm^{3+}	(0.6144, 0.3824)	1311
KMB: 6 mol% Sm^{3+}	(0.6195, 0.3751)	1256
KMB: 8 mol% Sm^{3+}	(0.6175, 0.3792)	1283

Conclusions

The unique single-phase orange-red glow producing these 2mol%, 4mol%, 6mol% and 8 mol% of Sm^{3+} ion doped in KMgBO_3 phosphor powders have been made utilised a standard solid-state reaction approach. A thorough examination of the crystal structure, its morphology, molecule vibrations, optical, emission, as well as

deteriorate life time features of produced phosphor powders were performed. According to XRD results, all of the produced phosphor powders crystallized in the $P2_13$ space group cubic system, with no extra spikes. It implies as all of specimens were synthesized in a single phase with no impurities. FTIR analysis revealed that the entire produced materials had B-O of trigonal BO_3 , B-O-B connections as well as metallic bonds. Absorption spectrums have been used to obtain the optical energy band gap standards. A emission spectrum were collected at 400nm, as well as emissions band were identified at 558, 608, 653 and 708 nm, correlating to the electronic shifts of Sm^{3+} ions $^4G_{5/2} \rightarrow ^6H_{5/2}$, $^6H_{7/2}$, $^6H_{9/2}$ and $^6H_{11/2}$ accordingly. This visible emission band was identified at 608nm across all of those emission bands. The level of emission increased till to 6 mol% with increasing Sm^{3+} ion concentration. However, when the doping concentration is further raised, the emission intensity dropped because of its concentration dampening effect. The CIE and CCT quantities were calculated using emission spectrum that proven, light it radiates in orange-red was warm. The deteriorating life time quantities of all Sm^{3+} added phosphor specimen were calculated. All of these findings indicate the phosphor specimens are well suited for orange components for white light emitting diodes as well as display purposes.

References

- [1] B.C. Jamalalah, N. Venkatramaiah, T.S. Rao, S.N. Rasool, B.N. Rao, D.V.R. Ram, A. S.N. Reddy, UV excited $SrAl_2O_4:Tb^{3+}$ nanophosphors for photonic applications, *Mater. Sci. Semicond. Process.* 105,104722(2020); <https://doi.org/10.1016/j.mssp.2019.104722>
- [2] B.C. Jamalalah, S.N. Rasool, Luminescence properties of $GdAl_3(BO_3)_4: Dy^{3+}$ phosphors for white-LEDs, *Mater. Today Proc.* 3,4019 (2016); <https://doi.org/10.1016/j.matpr.2016.11.066>
- [3] A. Pandey, V.K. Rai, $Pt^{3+}-Yb^{3+}$ codoped Y_2O_3 phosphor for display devices, *Mater. Res. Bull.* 57, 156 (2014); <https://doi.org/10.1016/j.materresbull.2014.04.071>
- [4] I. Gupta, S. Singh, S. Bhagwan, D. Singh, Rare earth (RE) doped phosphors and their emerging applications: A review, *Ceramics International* 47,19282 (2021); <https://doi.org/10.1016/j.ceramint.2021.03.308>
- [5] R. Dey, A. Pandey, V.K. Rai, The $Er^{3+}-Yb^{3+}$ codoped La_2O_3 phosphor in finger print detection and optical heating, *Spectrochim. Acta Part A* 128, 508 (2014); <https://doi.org/10.1016/j.saa.2014.02.175>
- [6] S. Som, V. Kumar, V. Kumar, M. Gohain, A. Pandey, M.M. Duvenhage, J.J. Terblans, B.C.B. Bezuidenhoud, H.C. Swart, Dopant distribution and influence of sonication temperature on the pure red

- light emission of mixed oxide phosphor for solid state lighting, *Ultrason. Sonochem.* 28, 79 (2016); <https://doi.org/10.1016/j.ultsonch.2015.07.003>
- [7] A. Pandey, V.K. Rai, V. Kumar, V. Kumar, H.C. Swart, Up-conversion based temperature sensing ability of $\text{Er}^{3+}\text{-Yb}^{3+}$ co-doped SrWO_4 : an optical heating phosphor, *Sens. Actuators B: Chem.* 209,352 (2015); <https://doi.org/10.1016/j.snb.2014.11.126>
- [8] V. Kumar, A. Pandey, S.K. Swami, O.M. Ntwaeaborwa, H.C. Swart, V. Dutta, Synthesis and characterization of $\text{Er}^{3+}\text{-Yb}^{3+}$ doped ZnO up-conversion nanoparticles for solar cell application, *J. Alloys Compd.* 766,429 (2018); <https://doi.org/10.1016/j.jallcom.2018.07.012>
- [9] R. Dey, A. Pandey, V.K. Rai, $\text{Er}^{3+}\text{-Yb}^{3+}$ and $\text{Eu}^{3+}\text{-Er}^{3+}\text{-Yb}^{3+}$ co-doped Y_2O_3 phosphors as optical heater, *Sens. Actuators B: Chem.* 190, 512 (2014); <https://doi.org/10.1016/j.snb.2013.09.025>
- [10] T.K. Pathak, A. Kumar, L.J.B. Erasmus, A. Pandey, E. Coetsee, H.C. Swart, R.E. Kroon, Highly efficient infrared to visible up-conversion emission tuning from red to white in Eu/Yb co-doped NaYF_4 phosphor, *Spectrochim. Acta Part A* 207, 23 (2019); <https://doi.org/10.1016/j.saa.2018.08.064>
- [11] A. Yousif, B.H. Abbas, V. Kumar, A. Pandey, H.C. Swart, Luminescence properties of Eu^{3+} activated Y_2O_3 red phosphor with incorporation of Ga^{3+} and Bi^{3+} trace hetero-cations in the Y_2O_3 lattice, *Vacuum* 155,73 (2018); <https://doi.org/10.1016/j.vacuum.2018.05.054>
- [12] A. Pandey, V. Kumar, S. Som, A. Yousif, R.E. Kroon, E. Coetsee, H.C. Swart, Photon and electron beam pumped luminescence of Ho^{3+} activated CaMoO_4 phosphor, *Appl. Surf. Sci.* 423, 1169 (2017); <https://doi.org/10.1016/j.apsusc.2017.06.326>
- [13] G.C. Gul, F. Kurtulus, RE (Y, Er, Gd, La, Nd, Sm, Dy)-doped SrBPO_5 colorful phosphors: definition of structural unit cell parameters and optical properties, *Optik* 139, 265 (2017); <https://doi.org/10.1016/j.ijleo.2017.03.110>
- [14] A. Pandey, V. Kumar, R.E. Kroon, H.C. Swart, Temperature induced upconversion behaviour of $\text{Ho}^{3+}\text{-Yb}^{3+}$ codoped yttrium oxide films prepared by pulsed laser deposition, *J. Alloys Compd.* 672, 190 (2016); <https://doi.org/10.1016/j.jallcom.2016.02.131>
- [15] A. Pandey, V.K. Rai, K. Kumar, Influence of Li^{+} codoping on visible emission of $\text{Y}_2\text{O}_3\text{:Tb}^{3+}, \text{Yb}^{3+}$ phosphor, *Spectrochim. Acta Part A* 118, 619 (2014); <https://doi.org/10.1016/j.saa.2013.08.109>

- [16] V. Vidyadharan, S. Sameera, K.G. Gopchandran, Luminescent properties of $\text{Li}_4\text{Ti}_5\text{O}_{12}:\text{Eu}^{3+}$ reddish-orange phosphors for WLED applications, *Mater. Today Proc.* 26, 117 (2020); <https://doi.org/10.1016/j.matpr.2019.05.447>
- [17] E. Sreeja, S. Gopi, V. Vidyadharan, P.R. Mohan, C. Joseph, N.V. Unnikrishnan, P. R. Biju, Luminescence properties and charge transfer mechanism of host sensitized $\text{Ba}_2\text{CaWO}_6:\text{Eu}^{3+}$ phosphor, *Powder Technol.* 323, 445 (2018); <https://doi.org/10.1016/j.powtec.2017.09.036>
- [18] E. Sreeja, V. Vidyadharan, S.K. Jose, A. George, C. Joseph, N.V. Unnikrishnan, P.R. Biju, A single-phase white light emitting Pr^{3+} doped Ba_2CaWO_6 phosphor: synthesis, photoluminescence and optical properties, *Opt. Mater.* 78, 52 (2018); <https://doi.org/10.1016/j.optmat.2018.02.003>
- [19] Z. Ju, R. Wei, X. Gao, W. Liu, C. Pang, Red phosphor $\text{SrWO}_4:\text{Eu}^{3+}$ for potential application in white LED, *Opt. Mater.* 33, 909 (2011); <https://doi.org/10.1016/j.optmat.2011.01.025>
- [20] Z.H. Ju, R.P. Wei, J.X. Ma, C.R. Pang, W.S. Liu, A novel orange emissive phosphor $\text{SrWO}_4:\text{Sm}^{3+}$ for white light-emitting diodes, *J. Alloys Compd.* 507, 133 (2010); <https://doi.org/10.1016/j.jallcom.2010.07.138>
- [21] D.singh, V. Tanwar, A. P. Samantilleke, B. Mari, S. Bhjagwan, P. S. Kadyan, I. Singh, Preparation and Photoluminescence Properties of $\text{SrAl}_2\text{O}_4:\text{Eu}^{2+}, \text{RE}^{3+}$ Green Nanophosphors for Display Device Applications, *J. Elect. Mate.* 2016, 45, 2718 (2016); <https://doi.org/10.1007/s11664-015-4318-z>
- [22] Y. Wang, G. Zhu, S. Xin, Q. Wang, Y. Li, Q. Wu, C. Wang, X. Wang, X. Ding, W. Geng, Recent development in rare earth doped phosphors for white light emitting diodes, *J. Rare Earths* 33,1 (2015); [https://doi.org/10.1016/S1002-0721\(14\)60375-6](https://doi.org/10.1016/S1002-0721(14)60375-6)
- [23] V. Vidyadharan, M.P. Remya, S. Gopi, S. Thomas, C. Joseph, N.V. Unnikrishnan, P.R. Biju, Synthesis and luminescence characterization of $\text{Sr}_{0.5}\text{Ca}_{0.5}\text{TiO}_3:\text{Sm}^{3+}$ phosphor, *Spectrochim. Acta Part A* 150, 419 (2015); <https://doi.org/10.1016/j.saa.2015.05.054>
- [24] A. Jha, B. Richards, G. Jose, T.T. Fernandez, P. Joshi, X. Jiang, J. Lousteau, Rare-earth ion doped TeO_2 and GeO_2 glasses as laser materials, *J. Prog. Mater. Sci.* 57, 1426 (2012); <https://doi.org/10.1016/j.pmatsci.2012.04.003>
- [25] G. Neelima, V.K. Kummara, N. Ravi, K. Suresh, S.N. Rasool, K. Tyagarajan, T.J. Prasad, Investigation of spectroscopic properties of Sm^{3+} -doped oxyfluorophosphate glasses for laser and display applications, *Mater. Res. Bull.* 110, 223 (2019); <https://doi.org/10.1016/j.materresbull.2018.10.026>

- [26] S. Thomas, R. George, S.N. Rasool, M. Rathaiah, V. Venkatramu, C. Joseph, N.V. Unnikrishnan, Optical properties of Sm^{3+} ions in zinc potassium fluorophosphate glasses, *Opt. Mater.* 36, 242 (2013); <https://doi.org/10.1016/j.optmat.2013.09.002>
- [27] S.N. Rasool, L.R. Moorthy, C.K. Jayasankar, Spectroscopic investigation of Sm^{3+} doped phosphate based glasses for reddish-orange emission, *Opt. Commun.* 311,156 (2013); <https://doi.org/10.1016/j.optcom.2013.08.035>
- [28] S. Thomas, S.N. Rasool, M. Rathaiah, V. Venkatramu, C. Joseph, N.V. Unnikrishnan, Spectroscopic and dielectric studies of Sm^{3+} ions in lithium zinc borate glasses, *J. Non-Cryst. Solids* 376, 106 (2013); <https://doi.org/10.1016/j.jnoncrysol.2013.05.022>
- [29] S. Xin, G. Zhu, The synthesis and photoluminescence properties investigation of a versatile phosphor $\text{Sr}_{10}[(\text{PO}_4)_{5.5}(\text{BO}_4)_{0.5}](\text{BO}_2): \text{Sb}^{3+}/\text{Eu}^{3+}/\text{Pr}^{3+}/\text{Dy}^{3+}$, *J. Lumin.* 181, 443 (2017); <https://doi.org/10.1016/j.jlumin.2016.09.040>
- [30] X. Zhang, F. Meng, W. Li, S.I. Kim, Y.M. Yu, H.J. Seo, Investigation of energy transfer and concentration quenching of Dy^{3+} luminescence in $\text{Gd}(\text{BO}_2)_3$ by means of fluorescence dynamics, *J. Alloys Compd.* 578, 72 (2013); <https://doi.org/10.1016/j.jallcom.2013.05.012>
- [31] W.R. Liu, C.-H. Huang, C.-P. Wu, Y.-C. Chiu, Y.-T. Yeh, T.-M. Chen, High efficiency and high color purity blue-emitting $\text{NaSrBO}_3:\text{Ce}^{3+}$ phosphor for near UV light-emitting diodes, *J. Mater. Chem.* 21, 6869 (2011); <https://doi.org/10.1039/c1jm10765h>
- [32] R. Wang, J. Xu, C. Chen, Luminescent characteristics of $\text{Sr}_2\text{B}_2\text{O}_5: \text{Tb}^{3+}, \text{Li}^+$ green phosphor, *Mater. Lett.* 68, 307 (2012); <https://doi.org/10.1016/j.matlet.2011.10.005>
- [33] R. Yu, N. Xue, H. Li, H. Ma, Synthesis, structure, and peculiar green-emitting of $\text{NaBaBO}_3: \text{Ce}^{3+}$ phosphor, *Dalton Trans.* 43, 10969 (2014); <https://doi.org/10.1039/c4dt00859f>
- [34] Z.-W. Zhang, Y. S. Peng, X.-H. Shen, J.-P. Zhang, S.-T. Song, Q. Lian, Enhanced novel orange red emission in $\text{LiSr}_{4-x}(\text{BO}_3)_3: x\text{Sm}^{3+}$ by K^+ , *J. Mater. Sci.* 49, 2534 (2014); <https://doi.org/10.1007/s10853-013-7948-7>
- [35] L. Wu, B. Wang, Y. Zhang, L. Li, H.R. Wang, H. Yi, Y.F. Kong, J.J. Xu, Structure and photoluminescence properties of a rare-earth free red-emitting Mn^{2+} -activated KMgBO_3 , *Dalton Trans.* 43, 13845 (2014); <https://doi.org/10.1039/c4dt01524j>

- [36] P. Ankoji, B.H. Rudramadevi, structural and luminescence properties of $\text{LaAlO}_3:\text{Sm}^{3+}$ nanophosphors synthesized via hydrothermal method, *Opt. Mater.*, 95, 109249 (2019); <https://doi.org/10.1016/j.optmat.2019.109249>
- [37] L.J.Q. Maia, A. Ibanez, L. Ortega, V.R. Mastelaro, A.C. Hernandez, Er:YAB nanoparticles and vitreous thin films by the polymeric precursor method, *J. Nanopart.Res.* 10, 1251 (2008); <https://doi.org/10.1007/s11051-007-9349-9>
- [38] E. Beregi, A. Watterich, L. Kovacs, J. Madarasz, Solid-state reactions in $\text{Y}_2\text{O}_3:3\text{Al}_2\text{O}_3:4\text{B}_2\text{O}_3$ system studied by FTIR spectroscopy and X-ray diffraction, *Vib. Spectrosc.* 22, 169 (2000); [https://doi.org/10.1016/S0924-2031\(99\)00078-8](https://doi.org/10.1016/S0924-2031(99)00078-8)
- [39] M. Jiao, C. Yang, M. Liu, Q. Xu, Y. Yu, H. You, Mo^{6+} substitution induced band structure regulation and efficient near-UV-excited red emission in $\text{NaLaMg}(\text{W}, \text{Mo})\text{O}_6:\text{Eu}$ phosphor, *Opt. Mater. Express* 7,2660 (2017); <https://doi.org/10.1364/OME.7.002660>
- [40] W.T. Carnall, P.R. Fields, K. Rajnak, Electronic energy levels in the trivalent lanthanide aquo ions. Pr^{3+} , Nd^{3+} , Pm^{3+} , Sm^{3+} , Dy^{3+} , Ho^{3+} , Er^{3+} and Tm^{3+} , *J. Chem. Phys.* 49,4424 (1968); <https://doi.org/10.1063/1.1669893>
- [41] R.V. Deun, K. Binnemans, C. Gorller-Walrand, J.L. Adam, Spectroscopic properties of trivalent samarium ions in glasses, *Proc. SPIE*, 3622, 175 (1999); <https://doi.org/10.1117/12.344508>
- [42] J.A. Wani, N.S. Dhoble, N.S. Kokode, S.J. Dhoble, Synthesis and photoluminescence property of RE^{3+} activated $\text{Na}_2\text{CaP}_2\text{O}_7$ phosphor, *Adv. Mater. Lett.* 5, 459 (2014); <https://doi.org/10.5185/amlett.2014.amwc.1211>
- [43] S.K. Sharma, S. Som, R. Jain, A.K. Kunti, Spectral and CIE parameters of red emitting $\text{Gd}_3\text{Ga}_5\text{O}_{12}:\text{Eu}^{3+}$ phosphor, *J. of Lumin.*, 159,317 (2015); <https://doi.org/10.1016/j.jlumin.2014.11.010>
- [44] M.N. Huang, Y.Y. Ma, X.Y. Huang, S. Ye, Q.Y. Zhang, The luminescence properties of Bi^{3+} sensitized $\text{Gd}_2\text{MoO}_6:\text{RE}^{3+}$ (RE = Eu or Sm) phosphors for solar spectral conversion, *Spectrochim. Acta Part A.*, 115,767 (2013); <https://doi.org/10.1016/j.saa.2013.06.111>